Femtosecond laser modification of titanium surfaces: direct imprinting of hydroxylapatite nanopowder and wettability tuning via surface microstructuring

Andrey A Ionin[1], Sergey I Kudryashov[1], Sergey V Makarov[1], Pavel N Saltuganov[1], Leonid V Seleznev[1], Dmitry V Sinitsyn[1], Evgene V Golosov[2], Artem A Goryainov[2], Yury R Kolobov[2], Kateryna A Kornieieva[2], Andrei N Skomorokhov[2] and Alexander E Ligachev[3]

[1] P N Lebedev Physical Institute RAS, Leninskiy prospect 53, 119991 Moscow, Russia
[2] Belgorod State University, Pobedy Street 85, 308015 Belgorod, Russia
[3] A M Prokhorov General Physics Institute RAS, Vavilova street 38, 119991 Moscow, Russia

E-mail: sikudr@lebedev.ru and kolobov@bsu.edu.ru

Abstract
Femtosecond laser modification of titanium surfaces was performed to produce microstructured hydrophilic and biocompatible surface layers. Biocompatible nano/microcoatings were prepared for the first time by dry femtosecond laser imprinting of hydroxylapatite nano/micropowder onto VT6 titanium surfaces. In these experiments HAP was first deposited onto the titanium surfaces and then softly imprinted by multiple femtosecond laser pulses into the laser-melted surface metal layer. The surface relief was modified at the nano- and microscales depending on the incident laser fluence and sample scanning speed. Wetting tests demonstrated that the wetting properties of the pristine Ti surface can be tuned through its laser modification in both the hydrophobic and hydrophilic directions.

1. Introduction

Titanium (Ti) implants are currently being key elements in repairing of bone defects in orthopedics [1, 2]. Modification of chemical composition and topography of Ti-implant surfaces enables, through biocompatibility and corrosion resistance, their medical functionality within living organisms to be varied [3–5].

Particularly, preliminary deposition of nanocrystalline hydroxylapatite $Ca_{10}(PO_4)_6(OH)_2$ (HAP) on Ti-implant surfaces provides biocompatible relief, which is necessary for bone tissue growth (osteointegration) and bioactivity owing to the calcium and phosphate HAP components [2, 5]. Recently, one approach to direct, controllable HAP deposition on Ti surfaces was attempted by their femtosecond (fs) laser irradiation at various incident laser fluences $F = 3$–10 J cm^{-2}

and surface scanning speeds of 0.2–1.8 mm s^{-1} within HAP water solutions of variable—from under- to supersaturated—concentrations, prepared as a mixture of $CaCl_2$ and Na_3PO_4 water solutions, using distilled water as a reference medium [6]. It was found that an increase of laser fluence with simultaneously decreasing scanning speed results in more distinct surface microstructures (characteristic dimensions ≈ 3 μm), comparing to lower fluences and higher scanning speeds, when mostly sub-micron surface microrelief emerges. The surface topography appeared to be almost independent of HAP concentrations, while its final chemical composition demonstrated some calcium and oxygen contents [6]. Hence, such rather severe fs-laser irradiation of Ti surfaces within the HAP water solutions has not provided observable HAP surface coatings, since stoichiometric HAP transfer from the solutions to the surface seems hardly probable through the high-intensity (10–100 TW cm^{-2}) fs-laser-induced breakdown and atomization of the intact HAP solution near the Ti surface.

Alternatively, surface biocompatibility of titanium implants can be tuned via changing their wetting characteristics, provided by topographical surface modification even without appreciable chemical composition alteration. As an example, multi-scale relief textures including micro- and nanoscale features were produced on Ti surfaces by multiple fs-laser pulses [7–12]. In this way, hydrophilic [13, 14] and superhydrophobic [15] titanium surfaces were fabricated, revealing direct correlation between wetting characteristics, surface relief features and bioactivity of various cell cultures of living body and pathogenic bacteria [13, 15].

In this letter we report a new principle of direct HAP deposition on Ti surfaces under dry conditions via mild fs-laser sputtering of a precoated poorly adhered HAP layer on its own Ti substrate, resulting also in nano- or nano/microstructuring of the substrate. Additionally, we have studied fs-laser nano- and microstructuring of bare Ti substrates and their resulting wetting characteristics.

2. Experimental details

In our experiments we used linearly polarized pulses of a regeneratively and multi-pass amplified Ti:Sa laser system (Avesta Project Ltd) at a central fundamental harmonic wavelength $\lambda_{las} \approx 744$ nm (FWHM parameter of ≈13 nm), pulse width τ_{las}(FWHM) ≈ 120 fs (in the region of laser–matter interaction), maximum pulse energy $E_{las} \approx 8$ mJ and a repetition rate of 10 Hz [16]. Laser energy was varied discretely and continuously by means of transmittive diffraction (binary attenuation in the range of 1.5–100%, Institute of Automatics and Electrometry, SB RAS) and reflective polarization (continuous attenuation in the range of 6–100%, Avesta Project Ltd) attenuators. Normally incident laser pulses characterized by a spatial TEM_{00} mode ($1/e^2$-beam diameter $2w_{las} \approx 8$ mm) were weakly focused in air into a 0.6 mm broad laser spot on a horizontal nanocrystalline (0.25 μm grain size) titanium VT6 slab surface with a pre-deposited 1 mm thick layer of HAP nanocrystallites (NIIEM RAMN), providing peak fluences

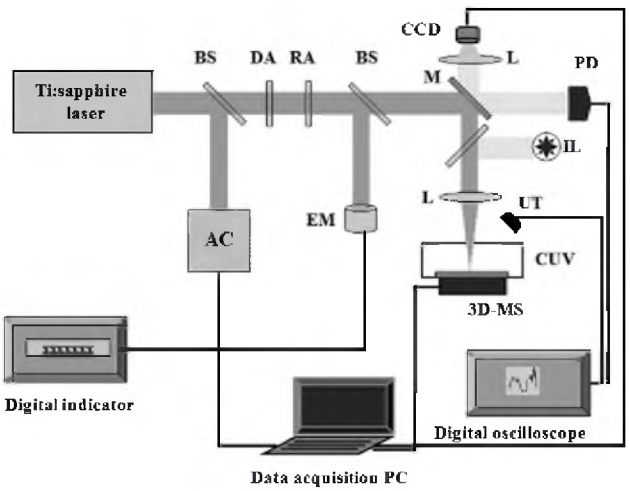

Figure 1. Experimental setup for femtosecond laser surface micro-processing: BS—beam splitter, AC—auto-correlator for laser pulsewidth measurements, DA, RA—variable diffractive and reflective energy attenuators, EM—thermocouple energy meter, M—mirror, L—focusing fused silica lens, CCD—charge-coupled device camera for surface imaging, PD—fast trigger silicon photodiode, IL—illumination lamp, CUV—cuvette for samples, 3D-MS—three-dimensional motorized micro-stage.

$F = 0.5$–2 J cm^{-2} in the pulse energy range of 0.5–3 mJ. The Ti samples were arranged in front of the laser focal point on a motorized 3D-stage and scanned in a number of patterns with different lines at different F and speeds of 6, 20 and 600 μm s^{-1} (figure 1). The resulting surface relief and its chemical compositions were characterized at 10 keV electron energy using a scanning electron microscope Quanta 600 FEG, equipped with an x-ray fluorescence (EDAX) analyzer (see EDAX spectra in figure 5). Wettability of the structured titanium surfaces was characterized using a sessile drop method, using distilled water drops (the typical volume 0.5 ± 0.05 μl) with dimensions much larger than the characteristic nano- and microtexture lengths. All specimens, including a reference polished titanium sample, were precleaned just before the tests with acetone to minimize chemical contamination of their surfaces. The tests were carried out at an ambient laboratory temperature. The equilibrium contact angles were measured after 2 s starting from water drop depositions. The contact angle has been measured using a high resolution, 8 Mpixel CCD camera with the accuracy ~3–5%, given by 5 independent measurements.

3. Experimental results and discussion

Upon fs-laser irradiation of the HAP-precoated Ti samples at $F \approx 0.5$ J cm^{-2} and scanning speed $\upsilon = 20$ μm s^{-1} ($N \approx 3 \times 10^2$) there are only laser-induced one-dimensional (1D) periodic nanostructures (LIPSS) with periods $\Lambda \approx$ 0.4–0.5 μm (figure 2(a)) well-oriented perpendicularly to the laser polarization, in agreement with previous observations for clean Ti surfaces [17], which were observed on the surface without any final HAP surface coating. At higher $F \approx 1$ J cm^{-2} and the same scanning speed LIPSS have

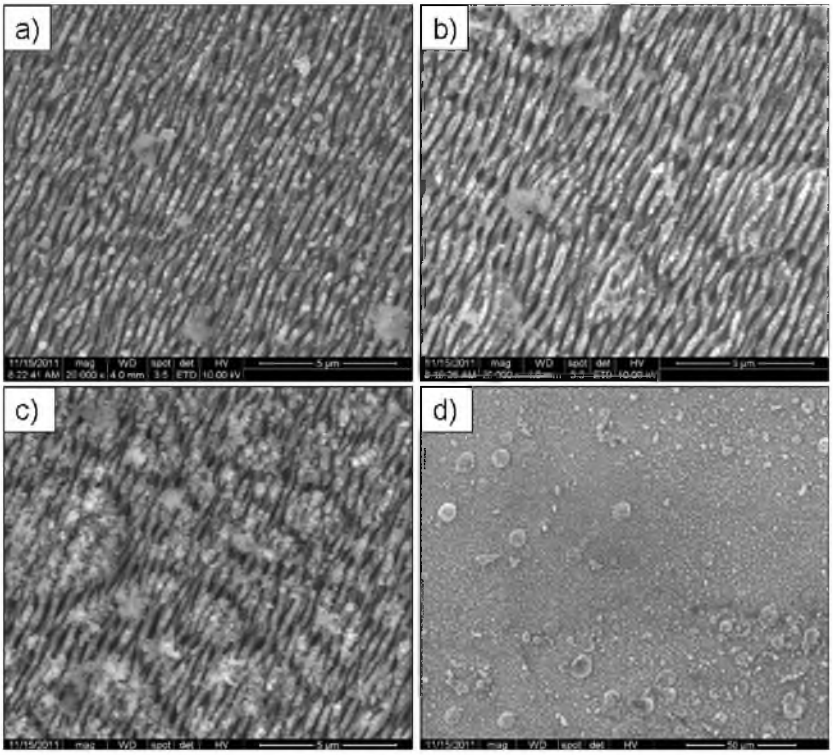

Figure 2. SEM images of the HAP-precoated Ti surface irradiated at $F = 0.5$ (a), 1 (b) and 2 (c), (d) J cm^{-2} for $\upsilon = 20$ μm s^{-1}.

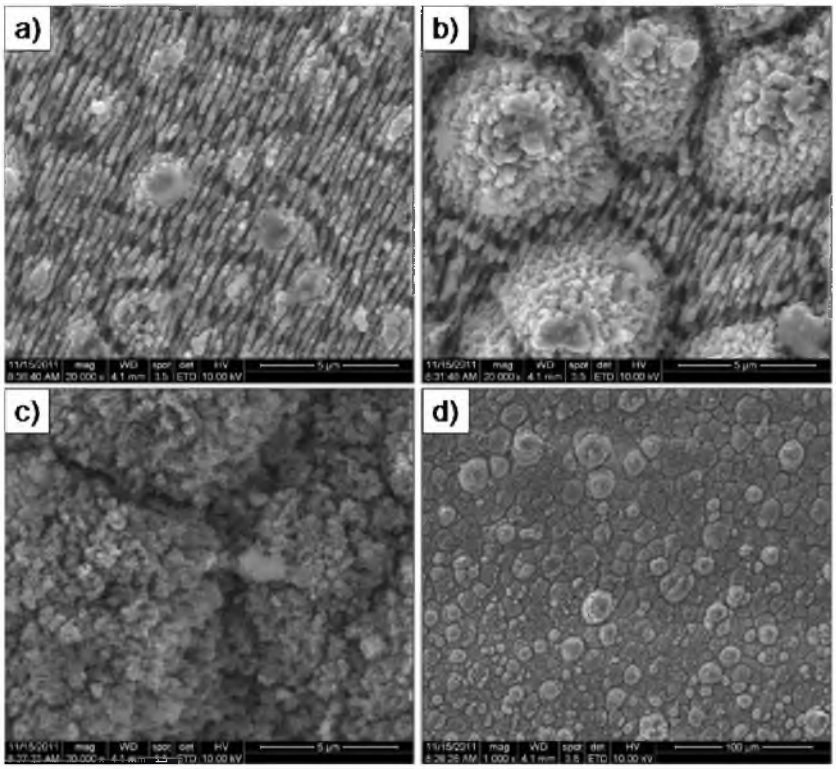

Figure 3. SEM images of the HAP-precoated Ti surface irradiated at $F = 0.5$ (a), 1 (b) and 2 (c), (d) J cm^{-2} for $\upsilon = 6$ μm s^{-1}.

the same periods $\Lambda \approx 0.4$–0.5 μm (figure 2(b)), however, HAP particulates start to appear on the surface. Then, at $F \approx 2$ J cm^{-2} 0.5 μm LIPSS are still present on the surface, which is now covered by larger (1–10 μm) HAP particulates (figures 2(c) and (d)). Real-time optical visualization shows that in this irradiation regime intense ablation of the upper

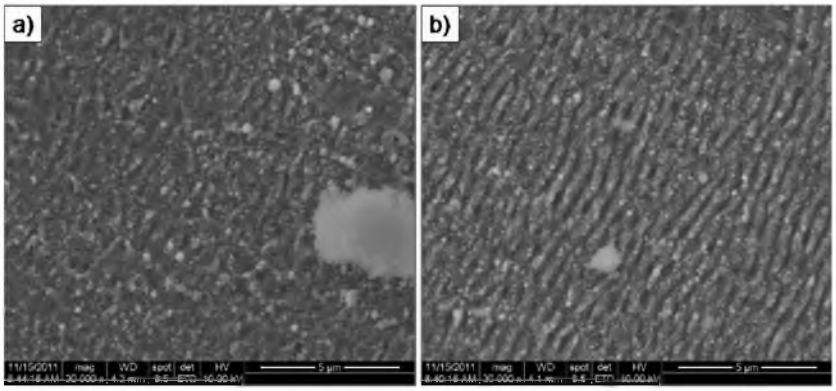

Figure 4. SEM images of the HAP-precoated Ti surface scanned forth (a) and forth/back (b) at $F = 2$ J cm^{-2} and $\upsilon = 600$ μm s^{-1}.

Table 1. Elemental composition of the precoated Ti surface after its fs-laser irradiation in the various regimes.

Parameter	Regime 1	Regime 2	Regime 3	Regime 4	Regime 5	Regime 6	Regime 7	Regime 8
F (J cm^{-2})	2. 1	1. 05	0. 525	2. 1	1. 05	0. 525	2. 1	2. 1
υ (μm s^{-1})	20	20	20	6	6	6	600	600
C (at.%)	3. 05		2. 50	3. 82	3. 53	1. 98	2. 85	2. 42
O (at.%)	30. 80		25. 08	42. 36	40. 84	26. 98	11. 00	10. 44
Al (at.%)	6. 80		7. 07	7. 53	6. 08	6. 91	8. 36	8. 34
P (at.%)	0. 39		0	0. 38	0. 40	0	0	0
Ca (at.%)	0. 42		0	0. 41	0. 51	0	0	0
Ti (at.%)	58. 55		65. 34	45. 51	48. 63	64. 12	77. 79	78. 8

HAP layer, which is accompanied by a visibly plasma spark and soudible shock wave emission, yields in blowing HAP off ahead of the moving laser spot stronger at higher F and less pronounced at lower F.

Again, at a scanning speed $\upsilon = 6$ μm s^{-1} ($N \approx 10^3$), and $F \approx 0.5$ J cm^{-2}, only LIPSS with periods $\Lambda \approx 0.4$–0.5 μm are present on the surface with minor HAP traces (figure 3(a)). Meanwhile, at higher $F \approx 1$ J cm^{-2} (figure 3(b)) there is a dense HAP layer composed of micron-sized particulates. Moreover, at $F \approx 2$ J cm^{-2} the surface is completely covered by HAP (figures 3(c) and (d)). Optical visualization shows almost no blow-off effect at $F \approx 0.5$ J cm^{-2}, while narrow and broad lines of the fs-laser irradiated Ti surface with plasma blown off HAP appear at $F \approx 1$ and 2 J cm^{-2}, respectively.

Finally, at scanning speed $\upsilon = 600$ μm s^{-1} ($N \approx 10$) and $F \approx 2$ J cm^{-2} the HAP-precoated Ti surface was scanned forth (figure 4(a)) or forth/back (figure 4(b)) to manage the blowing effect by making large inter-pulse steps of 60 μm in order to have HAP blown off back to the scanned line just behind the moving laser spot. However, under these fs-laser irradiation conditions only LIPSS with periods $\Lambda \approx 0.65$ μm without HAP are present on the surface after the forth/back scans (figure 4(b)) with LIPSS just appearing after the single forth scan (figure 4(a)). The previously revealed falling trend of the fluence dependence of the LIPSS periods (from ≈600 nm to ≈450 nm) on clean Ti surfaces [17] indicates, apparently, significant screening (scattering) of the fs-laser radiation by the HAP layer enabling only weak surface modification at the low transmitted laser fluences.

The EDAX chemical analysis results obtained for the different fs-laser scanned lines at low electron energies ≤6 keV to probe their thin surface layer (see figure 5), are summarized in table 1. Interestingly, some irradiation regimes—e.g., 1, 2, 4, 5—indicate the ratio Ca/P ≥ 1, which is reasonably similar to HAP with the initial composition $Ca_{10}(PO_4)_6(OH)_2$. Obviously, higher fs-laser fluences and longer exposure times (higher N, lower υ) typical for these

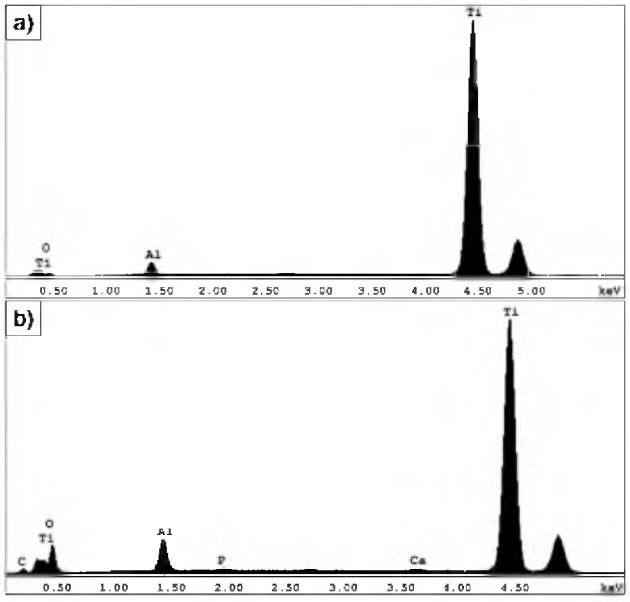

Figure 5. EDAX spectra of a pristine Ti surface (a) and a HAP-precoated Ti surface after their irradiation at $F \approx 1$ J cm^{-2} and $\upsilon = 6$ μm s^{-1}.

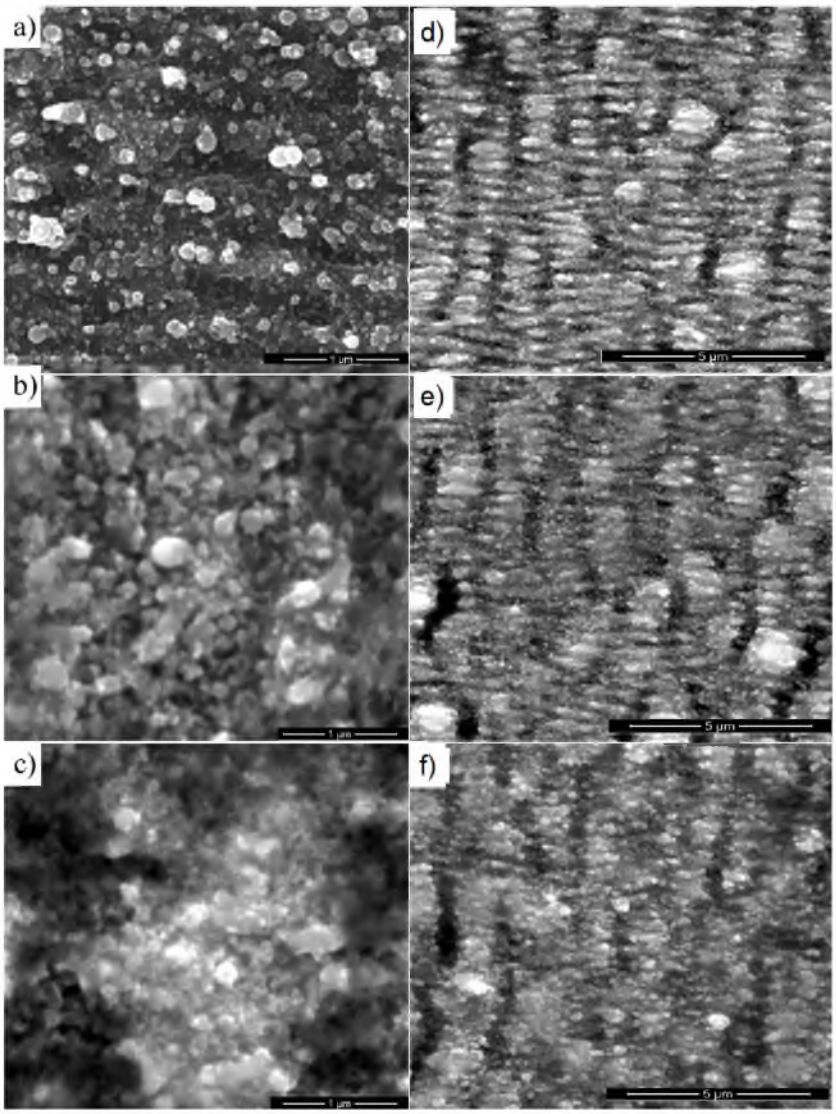

Figure 6. SEM images of the polished Ti surface irradiated at $F = 0.3$ (a), (d), 0.5 (b), (e), 1 J cm^{-2} (c), (f) for $\upsilon = 1000$ and 500 μm s^{-1}, respectively.

regimes, are more favorable for coating the Ti surfaces with HAP through longer fs-laser modification of the surfaces without the attenuating HAP layer, potentially, by producing deeper and more adhesive surface relief. Alternatively, more intense and longer fs-laser exposure may increase probability of the pre-deposited HAP nanocrystallites to be imprinted into the molten Ti surface (in this work, the incident fluences of 0.5–2 J cm^{-2} are higher than the melting and ablation threshold fluences for Ti, ≈0.05 and 0.3 J cm^{-2} [18], respectively), when the significant part of the pre-deposited screening HAP surface layer is blown off by previous fs-laser pulses.

The surface structuring of the polished untreated titanium was performed in air atmosphere at fluencies of 0.3, 0.5 and 1.0 J cm^{-2} and different laser scanning speeds in the range 20–1000 μm s^{-1}. Laser irradiation at $F \approx 0.3$, 0.5 and 1.0 J cm^{-2} and scanning speed $\upsilon = 1000$ μm s^{-1} produces irregular nanoscale relief with multiple sub-100 nm spherical particulates (figure 6), while at lower scanning speeds $\upsilon \leq$ 500 μm s^{-1} quasi-regular one-dimensional LIPSS with periods of $\Lambda \approx 0.4$–0.5 μm and larger perpendicular grooves appear simultaneously on the surface for all these fluences (figure 6). Furthermore, at even lower scanning speeds of 125–250 μm s^{-1} such grooves with the typical widths of ∼400–500 nm become more pronounced and separate the surface into micron-wide segments (figure 7). Later, at higher laser exposures, corresponding to the same fluences, but lower scanning speeds $\upsilon \leq 250$ μm s^{-1}, the grooves transform into distinct micro-columns (figure 7). The density of the columns increases for the decreasing scanning speeds, while their lateral dimensions increase with the increasing laser fluence (figure 7). These results are consistent with the trends observed during our fs-laser modification of HAP-precoated Ti samples above.

Additionally, our wetting tests have revealed that the contact angle for an untreated (polished) titanium surface can be tuned from its initial value of 71.2° in both—hydrophilic and hydrophobic—directions through its the laser-induced

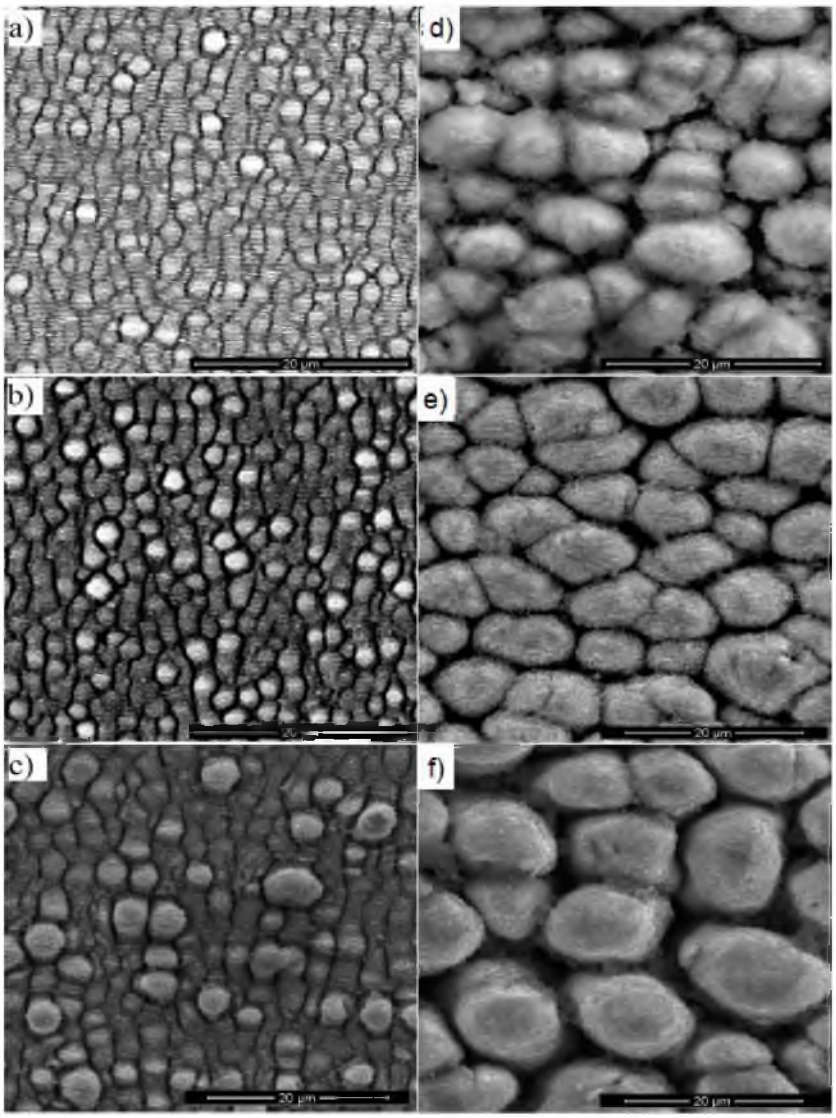

Figure 7. SEM images of the polished Ti surface irradiated at $F = 0.3$ (a), (d), 0.5 (b), (e), 1 J cm^{-2} (c), (f) for $\upsilon = 250$ and 18 μm s^{-1}, respectively.

surface modification. The contact angles measured on the laser-modified surfaces decreases up to 35°–60° at low laser scanning speeds (<20 μm s^{-1}) for all of the used laser fluences. In contrast, at high laser scanning speeds (>200 μm s^{-1}) the corresponding contact angles for the laser-modified surfaces are slightly higher or comparable to that of an untreated (polished) titanium surface at all of the used laser fluences. Clarification of the obvious correspondence between the topography of the fs-laser-modified surface and its wetting parameters is in progress.

In conclusion, in this work we have fabricated biocompatible hydroxylapatite surface coatings on titanium surfaces by imprinting a part of pre-deposited HAP layer into the surfaces during their multi-pulse femtosecond laser irradiation. We demonstrate the crucial fluence and scanning speed effects on HAP imprinting within this approach, developing functional properties of medical titanium implants. Femtosecond laser nano- and microstructuring was demonstrated to tune biocompatibility of titanium surfaces through changing their wetting properties either in hydrophobic, or in hydrophilic directions.

Acknowledgments

The authors acknowledge support of this work by the Russian Foundation for Basic Research (project nos 11-08-01165-a, 12-02-97528-r_center_a, 12-02-33045-mol-a-ved and 12-02-13506 OFI_m_RA), by Government Contract #16.740.11.0025 in the frame of Federal Target Program 'Scientific, academic and teaching staff of innovative Russian Federation' and State task of Ministry of Education and Science of Russian Federation #2.3315.2011, by the President grant no. 14.125.13.2470-MK, and by The Ministry of Education and Science of Russian Federation (project #8690).

References

[1] Yaszemski M J, Trantolo D J, Lewandrowski K-U, Hasirci V, Altobelli D E and Wise D L (ed) 2004 *Biomaterials in Orthopedics* (New York: Dekker)

[2] Kolobov Yu R 2009 *Nanotechnol. Russ.* **11/12** 758
[3] Vasil'ev M A, Beda B I and Gurin P A 2010 *The Physiological Response on the Surface State of.the Metallic Dental Implants* L'viv, Galdent (in Russian)
[4] Kolobov Yu R, Karlov A V, Bushnev L S and Sagimbaev E E 1998 *Acta Orthop. Scand.* **69** 48
[5] Fedorova M Z, Nadezdin S V, Kolobov Yu R, Ivanov M B, Pavlov N A and Zubareva E V 2009 *Bull. Exp. Biol. Med.* **148** 822
[6] Yang Y, Yang J, Liang C, Wang H, Zhu X and Zhang N 2009 *Opt. Express* **17** 21124
[7] Oliveira V, Ausset S and Vilar R 2009 *Appl. Surf. Sci.* **255** 7556
[8] Vorobyev A Y and Guo Ch 2007 *Appl. Surf. Sci.* **253** 7272
[9] Vorobyev A Y and Guo C 2006 *Opt. Express* **14** 2164
[10] Nayak B, Gupta M and Kolasinski K 2008 *Appl. Phys.* A **90** 399
[11] Liu X, Chu P K and Ding C 2004 *Mater. Sci. Eng.* R **47** 149
[12] Vorobyev A Y, Makin V S and Guo C 2007 *J. Appl. Phys.* **101** 034903
[13] Lawrence J, Hao L and Chew H R 2006 *Surf. Coat. Technol.* **200** 5581
[14] Bush J R, Nayak B K, Nair L S, Gupta M C and Laurencin C T 2011 *J. Biomed. Mater. Res.* **97B** 299
[15] Fadeeva E, Truong Kh, Stiesch M, Chichkov B N, Crawford R J, Wang J and Ivanova E P 2011 *Langmuir* **27** 3012
[16] Alekhin A A *et al* 2010 *Laser Phys. Lett.* **7** 463
[17] Golosov E V, Ionin A A, Kolobov Yu R, Kudryashov S I, Ligachev A E, Novoselov Yu N, Seleznev L V and Sinitsyn D V 2011 *JETP* **113** 14
[18] Ye M and Grigoropoulos C P 2001 *J. Appl. Phys.* **89** 5183